Physicochem. Probl. Miner. Process. 53(1), 2017, 110−120

www.minproc.pwr.wroc.pl/journal/

Physicochemical Problems of Mineral Processing

ISSN 1643-1049 (print)
ISSN 2084-4735 (online)

Received February 21, 2016; reviewed; accepted May 9, 2016

FEATURES OF DISTRIBUTION OF URANIUM AND THORIUM IN RED MUD

Hannian GU[*], Ning WANG[*], Yongqiong YANG[**], Chengdong ZHAO[*,*], Shanshan CUI[*,***]**

[*] Key Laboratory of High-temperature and High-pressure Study of the Earth's Interior, Institute of Geochemistry, Chinese Academy of Sciences, Guiyang 550081, China, guhannian@vip.gyig.ac.cn
[**] School of Geographic and Environmental Sciences, Guizhou Normal University, Guiyang, 550001, China
[***] University of Chinese Academy of Sciences, Beijing 100049, China

Abstract: Natural radioactive elements such as uranium and thorium restrict the use of red mud as building materials or additives, and may cause environmental problems. The distribution features of U and Th in red mud was studied from micro and macro analysis, using EPMA, LA-ICP-MS, and methods of mineralogy and beneficiation. Based on the micro-area scanning analysis, main chemical compositions in red mud, such as Ca, Al, Si, Na, and K are dispersive while Fe and Ti mainly tend to concentrate in granular phases. Based on the in-situ analysis, the distribution of main elements and most trace elements in micro-zone of red mud was homogeneous. In micro-zone area, the variation tendency of thorium content was similar with Y in red mud samples. By means of the methods of mineralogy and beneficiation, red mud samples were separated into different fractions. U and Th tend to be enriched in the low density fraction of the red mud. Th presented a high concentration in the finest particle size fractions of the red mud. Neither U or Th was regularly distributed in various magnetic red mud fractions. Thorium fingerprint peaks were determined in perovskite by EDX under TEM, which is proposed to be one of the radioactivity sources in Bayer red mud.

Keywords*: red mud, uranium, thorium, distribution, perovskite*

Introduction

Red mud is the main waste discharged during the alumina production. The utilization of red mud is realistically a significant problem in the alumina industry (Samal et al., 2013). Approximately 90% of alumina in the world is obtained by the Bayer process, while most local bauxite ores in China are low grade, diaspore type bauxite, which are effective for the sintering alumina process (Liu et al., 2007; 2009; Zhang et al., 2014). In China red mud residues are generally classified as Bayer red mud (BRM) and red mud from sintering alumina process (RMS) (Gu and Wang, 2013). The treatment and

http://dx.doi.org/10.5277/ppmp170109

disposal of red mud has posed a huge challenge not only for the alumina plants but also for the alumina industry. Red mud may lead to environmental pollution, for example, the dam of the red mud reservoir in Ajka (Hungary) which collapsed in October, 2010, causing rivers and land contamination (Gelencser et al., 2011; Ruyters et al., 2011; Kovacs et al., 2012).

Natural radioactive elements, uranium and thorium from bauxite ore, restrict the use of red mud as building materials or additives. It is reported that more than 80% of thorium and uranium in the bauxite are concentrated in red mud (Adams and Richardson, 1960a). Thorium in bauxites is associated mainly with accessory minerals inherited by the bauxites from the parent rocks, and uranium is mainly absorbed by clay minerals (Parshakov et al., 1977). The amount of radioactive elements in bauxites depends directly on the amounts of certain trace elements (zirconium, niobium etc.) and rare earth elements (mainly the cerium group) in them (Parshakov et al., 1978). In Surinam bauxite, thorium occurs in finer grained particles than uranium (Adams and Richardson, 1960b). It is unquestionable that red mud generally contains concentrations of thorium and uranium greater than the bauxites average. The radionuclide concentration of red mud significantly exceeds the world average for building materials. Red mud residues from Shandong (Zhao et al., 2009), Guizhou (Gu et al., 2012), and Hungary (Somlai et al., 2009), were reported to not meet the regulations of safety limits for radioactivity as construction materials directly.

It is previously reported that the possible forms of occurrence of U and Th in red mud was complex investigated by the modified Tessier's sequential extraction procedure (Gu and Wang, 2013). The aim of the present work is to disclose the distribution features of U and Th in both BRM and RMS from microscopic and macroscopic aspects. For micro aspect, the distribution and relationship between radioactive elements and some other chemical composition in red mud were analyzed. For macro aspect, the method of mineralogy and beneficiation was used to seek the relations of U and Th with density, particle size, electromagnetic properties of red mud particles. Contents of U and Th in some heavy minerals from red mud are also discussed in this study.

Materials and methods

Materials

Red mud samples used in this study, including Bayer red mud (BRM) and red mud from sintering alumina process (RMS), were obtained from Guizhou Enterprise of China Aluminum Co., Ltd. (GZHE).

Experimental

The micro-area scanning analysis of radioactive elements and the main chemical composition in red mud were conducted by Shimadzu EPMA-1600 (Shimadzu

Corporation, Japan) electron probe micro-analyzer (EPMA), and energy-dispersive X-ray spectroscopy analysis was carried out by Genesis EDAX. In-situ analyses of BRM and RMS were conducted by a Laser Ablation Inductively Coupled Plasma Mass Spectrometer (LA-ICP-MS), with the laser spot of 44 μm. Twelve points were collected from each sample.

Through the method of mineralogy and mineral processing technology, such as gravity dressing, particle-size classification and electromagnetic separation, the red mud samples were separated into different fractions. Gravity dressing was performed using water as medium to obtain three different density fractions. In order to separate red mud into different particle-size fractions, 500 g red mud sample was added to 5 dm^3 of distilled water and stirred to form a slurry, from which four fractions were obtained by wet sieving. Red mud under 20 μm fraction was separated into 5 different electromagnetic fractions by using a modified Frantz Isodynamic Magnetic Separator according to different current intensities. The distribution and characteristics U and Th in these different fractions were investigated to seek their relations with density, particle size, electromagnetic properties of red mud. Contents of U, Th in all samples before and after separation were analyzed by a Quadrupole Inductively Coupled Plasma Mass Spectrometer (ICP-MS, ELAN DRC-e, PerkinElmer). A Malvern Mastersizer 2000 laser scattering particle size distribution analyzer was used to determine the particle size distribution of the red mud samples. A multi-channel gamma spectrometer (Canberra S-100) with a high purity germanium (HPGe) detector was used to determine the specific activity of original red mud samples and various fractions.

For microscope observation of heavy minerals in Bayer red mud, samples were fixed on a copper supporting net, coated with graphite for observation and identification on a TEM instrument (JEM-2000FX, Japan) equipped with EM-ASID20 scanning and imaging system and an energy dispersive spectroscope (EDS, Oxford Link ISIS) at a maximal accelerating voltage of 200 kV.

Results and discussion

Micro-area scanning analysis

Back scattered electron (BSE) images and elemental distributions of Ca, Al, Si, Na, K, Fe, Ti, and Th of Guizhou Bayer red mud were analyzed (Fig. 1). It shows that the main chemical compositions in red mud, such as Ca, Al, Si, Na, and K were dispersive. Calcium was liable to concentrate highly in some larger size phases, while Al and Si were more dispersive. Na and K had a very similar distribution. As expected, Fe and Ti concentrated mainly in the some phases with granular shape. Thorium was not detected in the studied micro-zone, possibly due to the concentration of Th is lower than the detection limit of the instrument.

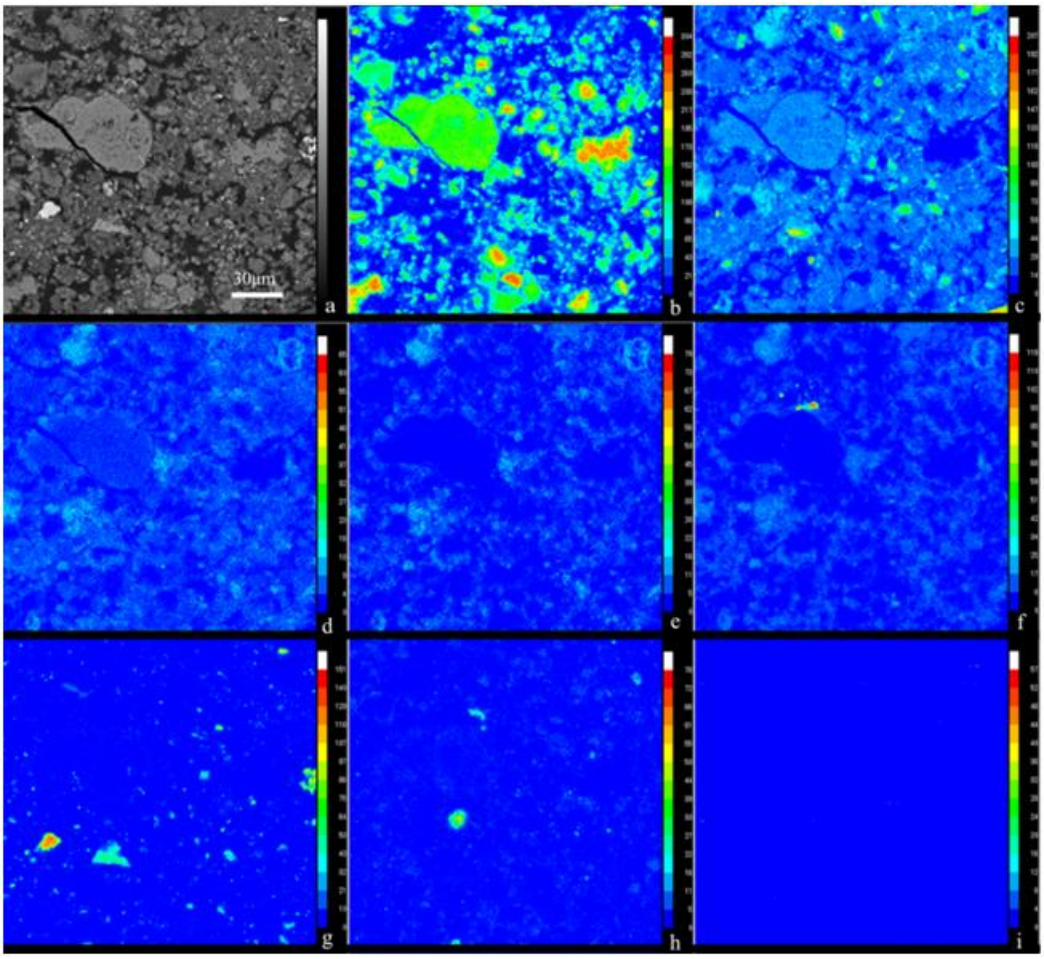

Fig. 1. BSE images of Guizhou Bayer red mud (a), and elemental distributions of Ca(b), Al(c), Si(d), Na(e), K(f), Fe(g), Ti(h), Th(i)

In-situ analysis

In-situ analyses of BRM and RMS were conducted by LA-ICP-MS, and 12 points were collected from each sample (Table 1). Most of the main elements in each micro-zone of both BRM and RMS are homogeneous, and the distribution of main elements does not relate to the contents of U or Th. In agreement with the micro-area scanning analysis, Fe and Ti in Bayer red mud tends to concentrate in some micro-areas. For Fe the maximum amount (11.6%) is 2.5-fold greater than the minimum (4.49%), and for Ti the maximum amount (7.52%) is twice more than the minimum (3.60%).

Table 1. Major chemical composition of red mud samples in micro zone (wt%)

Samples	Al_2O_3	SiO_2	FeO	CaO	TiO_2	Na_2O	K_2O	MgO	P_2O_5	MnO	Th ($\mu g\ g^{-1}$)	U ($\mu g\ g^{-1}$)
BRM-01	25.2	21.7	6.23	25.4	5.41	10.4	3.16	1.31	0.34	0.015	119	36.2
BRM-02	20.0	17.6	4.49	40.6	3.60	9.29	2.57	0.83	0.32	0.011	88.8	30.6
BRM-03	25.9	21.8	6.12	24.5	4.86	11.2	3.15	1.27	0.31	0.016	109	38.5
BRM-04	28.0	22.0	6.67	21.3	4.12	11.2	3.57	2.21	0.22	0.018	108	30.5
BRM-05	26.5	21.2	7.03	23.7	5.26	10.7	3.14	1.26	0.26	0.018	119	30.0
BRM-06	26.8	22.3	6.73	22.2	5.19	11.2	3.18	1.15	0.33	0.016	123	37.5
BRM-07	19.8	19.5	4.82	36.3	7.52	7.06	2.18	0.86	0.40	0.013	257	40.2
BRM-08	25.9	19.1	8.42	25.3	5.34	9.67	2.79	2.10	0.40	0.020	112	43.0
BRM-09	26.2	21.8	6.58	23.5	5.62	10.8	3.21	1.13	0.26	0.015	126	35.4
BRM-10	23.9	19.1	6.40	30.8	5.72	9.21	2.50	0.92	0.52	0.015	120	43.1
BRM-11	25.2	22.6	11.6	18.9	4.61	11.6	3.57	0.96	0.24	0.020	116	32.0
BRM-12	25.9	22.5	6.23	23.4	5.29	11.4	3.31	0.97	0.24	0.014	117	36.6
RMS-01	17.3	19.5	11.2	36.2	3.85	6.35	2.77	1.52	0.27	0.032	91.7	42.4
RMS-02	10.1	22.3	10.1	44.7	4.35	4.26	1.22	1.65	0.27	0.032	104	27.7
RMS-03	4.95	23.6	13.6	46.5	3.31	4.42	1.22	1.01	0.34	0.031	121	32.8
RMS-04	8.66	20.2	12.6	45.4	4.95	4.28	1.18	1.40	0.27	0.026	96.1	36.8
RMS-05	7.56	23.6	11.2	45.2	4.20	4.11	1.40	1.37	0.30	0.024	123	33.6
RMS-06	9.03	21.7	12.1	44.6	4.13	4.51	1.36	1.24	0.34	0.026	107	39.4
RMS-07	3.36	26.5	7.19	52.7	2.82	3.91	1.03	0.95	0.42	0.018	171	20.6
RMS-08	7.03	21.8	13.3	43.7	5.09	4.58	1.41	1.62	0.29	0.031	104	31.8
RMS-09	4.52	24.4	12.7	45.4	4.48	4.47	1.12	1.42	0.39	0.032	132	46.4
RMS-10	8.38	20.8	18.0	40.8	3.80	4.03	1.56	1.38	0.31	0.055	86.3	34.4
RMS-11	7.97	22.5	14.1	43.1	4.04	4.43	1.34	1.20	0.35	0.026	107	34.6
RMS-12	18.1	19.2	12.9	36.7	4.69	4.04	1.90	1.19	0.28	0.025	99.2	39.7

BRM: Bayer Red Mud; RMS, Red Mud from Sintering process

The distribution of most trace elements in the micro-zone of red mud is also homogeneous, and they do not distinctly relate to U. It is reported that Th correlated well with rare earth elements (REEs), and its leaching trend was similar to the total REEs in both BRM and RMS (Gu and Wang, 2013). From the micro-zone analysis of

12 points in BRM, it is found that contents of Y and Nb increased obviously with the increasing of the Th contents, while contents of Sc decreased slightly with the increasing of the contents of Th, while contents of U, W and Ta almost kept stable with the increasing of the contents of Th (Fig. 2a). Meanwhile, in micro-zone area of RMS contents of Y(obviouly) and Sc (slightly) increased with the increasing Th contents while contents of Nb and Ta decreased slightly with the increasing contents of Th. The contents of U and W were stable with the increasing Th contents (Fig. 2b).

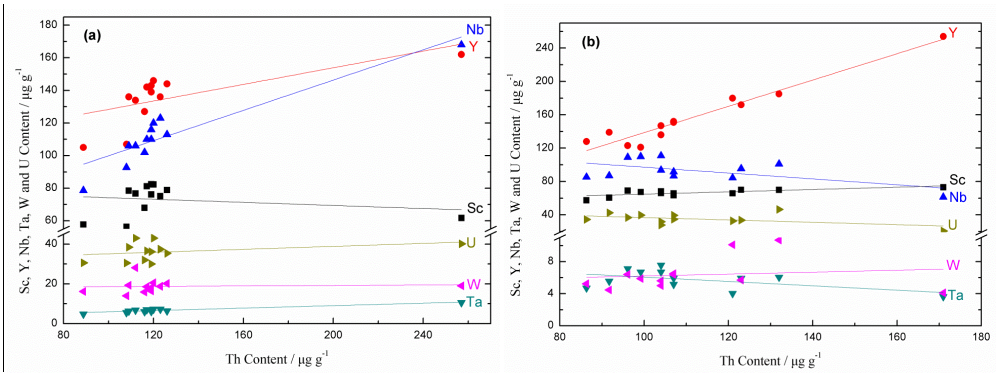

Fig. 2. Correlation of Th content vs content of other metals in micro-zone of BRM (a) and RMS (b)

Distribution of different density red mud fractions

For practical applications, to investigate the relationship with radioactive elements and different red mud fractions and to find the regular pattern of radioactive elements in different fractions, may be a precondition to separate the high-radio content fraction from red mud. Uranium and thorium are present in reasonably high concentrations in such heavy minerals as uraninite, monazite (Akinci and Artir, 2008), and zircon (Huang et al., 2009). The relationship between radioactive elements and the different fractions of red mud from the macro aspect was investigated in this study. Original red mud was separated into different density fractions using gravity separation method: (A) heavy fraction, 1% wt, (B) sub-heavy fraction, 10% wt, and (C) light fraction (the remaining fraction), ca. 80% wt. Uranium, Th, and some other elements that have related geochemistry properties were analyzed by ICP-MS in heavy fraction, light fraction, as well as original sample (Table 2). Generally, heavy minerals should be enriched in a heavy red mud fraction. Zircon is a typical heavy mineral, which tends to enter the heavy fraction. From Table 2, it is clear that the characteristic elements Zr and Hf in the heavy fraction were in higher concentration than those in the original red mud and light fraction, indicating that zircon was enriched in the heavy fraction. Scandium, Y, REEs, U and Th, did not have a similar tendency to enrich in the heavy fraction. Therefore, the heavy fraction was rich in heavy minerals, like zircon, which contains lower amount of U and Th than original red mud.

Contents of U and Th in original red mud is higher than these in the heavy fraction and lower than in the light fraction. This results can be identified by the specific activity analysis for different density fractions. The radioactive specific activity of each density fractions was determined. Internal exposure index (I_{Ra}) and external exposure index (I_{γ}) were calculated based on the data of radioactive specific activity (Gu et al., 2012). From Table 3, I_{Ra} and I_{γ} of original red mud sample are lower than those of light fraction and higher than those of heavy fraction. It seems that the light fraction contains more uranium and thorium than the heavy fraction does. The conclusion that U and Th tend to enrich in light fraction rather than heavy fraction is opposite to some points proposed before that consider that U and Th come from heavy minerals in red mud.

Table 2. U and Th contents of different density red mud fractions (μg g^{-1})

	Zr	Hf	Sc	Y	REEs	Th	U
Heavy fraction	2240	60.2	38.0	83.2	468	72.0	20.4
Light fraction	1250	37.9	71.8	138	1019	159	31.3
Original sample	2020	33.0	65.5	134	1237	102	25.0

Table 3. Radioactivity level of different density red mud fractions

	Specific activity (Bq kg^{-1})			I_{Ra}	I_{γ}
	^{226}Ra	^{232}Th	^{40}K		
Heavy fraction	268.0±5%	342.3±9%	354.6±7%	1.34	2.13
Light fraction	367.2±6%	445.3±10%	582.6±8%	1.84	2.82
Original sample	350.4±6%	414.0±10%	583.0±8%	1.75	2.68

Distribution of different particle size red mud fractions

It is known that in red mud some elements contents differ with different particle sizes. For example, physical separation methods was used to reduce chlorine in red mud for cement industry because the chlorine contents vary in different particle size fractions (Hyun et al., 2005). Iron, Si, and Ca are the three dominating components in the large particles (≥ 0.075 mm) from the raw red mud (Liu et al., 2011). It is necessary to find features of distribution of radioactive elements in different particle size red mud fractions. As described, red mud is classified into four fractions, fraction 1 (54~97 μm), fraction 2 (38.5~54 μm), fraction 3 (20~38.5 μm), and fraction 4 (< 20μm). Particle analysis shows that the four red mud particle size fractions are with a volume average diameter D[4,3] of 59.633μm, 37.895μm, 33.513μm, and 4.119 μm (Fig. 3), implying a reliable separation. Table 4 gives contents of U, Th, and other elements for contradistinctive study. It looks like that Th together with REEs was lightly enriched in the finest fraction (fraction 4). As discussed, this is possibly because REEs and thorium have similar geochemical properties. Scandium and Y have similar distribution, with a consistent conclusion from micro-zone analysis. All

the U contents in different particle size fractions were higher than these in original red mud, which may due to the uncertainty of the red mud or fraction samples. However, from the data it can be observed that distribution of U was irregular in different particle size fractions.

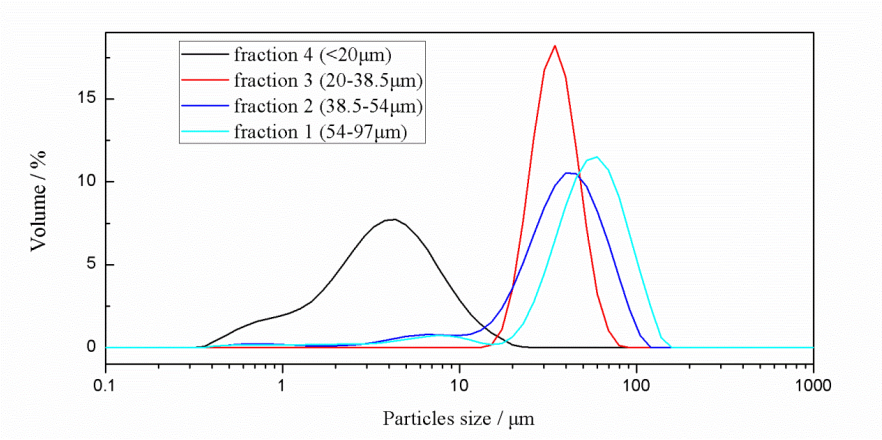

Fig. 3. The distribution of different particle size red mud fractions

Table 4. U and Th contents of different particle size red mud fractions (μg g^{-1})

	Zr	Hf	Sc	Y	REEs	Th	U
Fraction 1 (54–97 μm)	973	25.8	55.0	89.8	738	81.9	28.0
Fraction 2 (38.5–54 μm)	1210	31.8	58.9	94.5	693	78.2	28.5
Fraction 3 (20–38.5 μm)	2010	46.8	65.3	109	752	84.9	30.2
fraction 4 (< 20 μm)	1320	33.1	80.5	149	1106	120	27.3
Original sample	1290	35.9	82.0	129	908	99.9	26.1

Distribution of different electromagnetic red mud fractions

The iron minerals in red mud can be efficiently separated by magnetic separation even if the precipitate is very fine (Li et al., 2011). Electromagnetic method was applied in this study for mineral separation because red mud contains some magnetic minerals, like monazite, a kind of weak magnetic mineral. The ICP-MS data of the five fractions were obtained in another batch, so there were some uncertainties compared to the original red mud data. However, the content data of the magnetic red mud fractions can explain some phenomena. From the five different intensity magnetic fractions (Table 5), the non-magnetic fraction had higher concentration of Zr and Hf, indicating that non-magnetic mineral, zircon, was concentrated in this fraction. Generally, distributions of U and Th were irregular in different magnetic fractions of red mud. Uranium and Th were not enriched in any fraction. In this case the radioactive components cannot be separated by the magnetic method.

Table 5. U and Th contents of different electromagnetic red mud fractions (μg g^{-1})

	Zr	Hf	Sc	Y	REEs	Th	U
Strong magnetic fraction	1128	28.3	58.3	147	742	81.5	24.6
Sub-Strong magnetic fraction	1114	29.4	65.6	118	744	85.7	28.2
Medium magnetic fraction	1028	28.9	65.2	112	719	82.9	28.9
Weak magnetic fraction	1058	28.8	63.0	106	678	78.4	27.9
Non-magnetic fraction	2151	50.8	50.9	87.0	588	66.6	23.2
Original sample (< 20μm)	1320	33.1	80.5	149	1106	120	27.3

Composition of heavy minerals in red mud

Composition of several heavy minerals in Bayer red mud was investigated by EDX under TEM. It is not obvious that heavy minerals, like monazite, zircon and phosphate minerals, contain U or Th. However, some of the perovskite minerals contain fingerprint peaks of EDX (Fig. 4). From the EDX pattern, some of the perovskite minerals also contain other elements, like Na, Al, Si, and Sr. The Th-containing perovskite can be easily found in fraction 4 (particle size less than 20 μm). It is roughly estimated that 10-30% of perovskite minerals found under TEM contain Th, indicating that perovskite is one of the radioactivity sources in Bayer red mud. Perovskite is commonly present in red mud in China due to the addition of lime during the Bayer process (Liu et al., 2007; Grafe et al., 2011). Perovskite is proposed to be a kind of new formed phase in the Bayer process based on titania and calcium oxide (Klauber et al., 2011). The position of thorium in perovskite crystal is unclear. From this study, perovskite separation is proposed to be a promising method that can reduce the radioactivity of red mud.

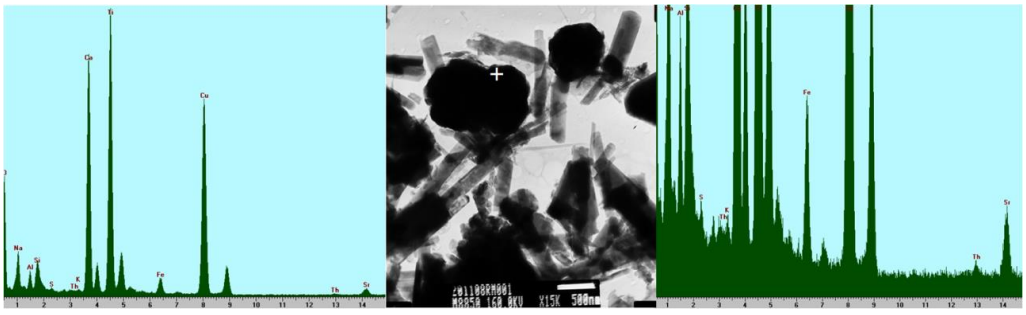

Fig. 4. Perovskite and its EDX analysis in Bayer red mud

Conclusions

Ca, Al, Si, Na, and K in Bayer red mud were dispersive, while Fe and Ti mainly concentrated in granular phases. In micro-zone areas of red mud, the distribution of main elements and most trace elements was homogeneous, and none of the main

elements related to the contents of U or Th. Some elements contents correlated with Th which had a positive variation tendency with Y and Nb in Bayer red mud, and it also had a positive variation tendency with Sc and Y and a negative variation tendency with Nb and Ta in red mud from sintering alumina process.

Contents of U and Th in the light fraction (accounting for 80 wt%) were higher than these in original red mud, while contents of U and Th in heavy fraction (accounting for 1wt%) were lower than these in original red mud. Distribution of U was irregular in different particle size fractions, while Th mildly enriched in small size fraction (less than 20μm). Thorium peaks were determined in perovskite, which was proposed to be one of the radioactivity sources in Bayer red mud. Physical separation does not seem to be an ideal approach to separate or reduce the radioactive components.

Acknowledgements

Authors would like to acknowledge the financial support of the National Natural Science Foundation of China (Grant No. 41402039), Guizhou Provincial Science and Technology Foundation (No. J [2012] 2329; No. J [2014] 2130), Doctoral Program Foundation of Guizhou Normal University, and Frontier Field Project of Institute of Geochemistry, Chinese Academy of Sciences (Y3CJ007000). H. Gu is thankful to the China Scholarship Council.

References

ADAMS J.A.S., RICHARDSON K.A., 1960a, *Radioactivity of aluminum metal*, Economic geology, 55, 1060-1063.

ADAMS J.A.S., RICHARDSON K.A., 1960b, *Thorium, uranium and zirconium concentrations in bauxite*, Economic geology, 55, 1653-1675.

AKINCI A., ARTIR R., 2008, *Characterization of trace elements and radionuclides and their risk assessment in red mud*, Materials Characterization, 59, 417-421.

GELENCSER A., KOVATS N., TUROCZI B., ROSTASI A., HOFFER A., IMRE K., NYIRO-KOSA I., CSAKBERENYI-MALASICS D., TOTH A., CZITROVSZKY A., NAGY A., NAGY S., ACS A., KOVACS. A., FERINCZ A., HARTYANI Z., POSFAI M., 2011, *The red mud accident in Ajka (Hungary): Characterization and potential health effects of fugitive dust*, Environmental Science & Technology, 45, 1608-1615.

GRAFE M., POWER G., KLAUBER C., 2011, *Bauxite residue issues: III. Alkalinity and associated chemistry*, Hydrometallurgy, 108, 60-79.

GU H., WANG N., 2013. *Leaching of uranium and thorium from red mud using sequential extraction methods*, Fresenius Environmental Bulletin, 22(9a), 2763-2769.

GU H., WANG N., LIU S., 2012, *Radiological restrictions of using red mud as building material additive*, Waste Management & Research, 30(9): 961-965.

HUANG Y., WANG N., WAN J., LIN J., LIU B., GU H., LI H., TIAN Y., 2009, *Comprehensive utilization of red mud and control techniques of radioactive issues*, Bulletin of Mineralogy, Petrology and Geochemistry, 28(2),128-130 (in Chinese).

HYUN J., ENDOH S., MASUDA K., SHIN H., OHYA H., 2005, *Reduction of chlorine in bauxite residue by fine particle separation*, International Journal Mineral Processing, 76, 13-20.

KLAUBER C., GRAFE M., POWER G., 2011, *Bauxite residue issues: II. options for residue utilization*, Hydrometallurgy, 108, 11-32.

KOVACS T., SAS Z., SOMLAI J., JOBBAGY V., SZEILER G., 2012, *Radiological investigation of the effects of red mud disaster*, Radiation Protection Dosimetry, 152, (1-3), 76-79.

LI Y., WANG J., WANG X., WANG B., LUAN Z., 2011, *Feasibility study of iron mineral separation from red mud by high gradient superconducting magnetic separation*, Physica C, 471, 91-96.

LIU W., YANG J., XIAO B., 2009, *Review on treatment and utilization of bauxite residues in China*, International Journal of Mineral Processing 93, 220-231.

LIU W., ZHANG X., JIANG W., ZHU X., YANG J., 2011, *Study on particle-size separation pretreatment of Bayer red mud*, Chinese Journal of Environmental Engineering, 5(4), 921-934 (in Chinese).

LIU Y., LIN C., WU Y., 2007, *Characterization of red mud derived from a combined Bayer Process and bauxite calcination method*, Journal of Hazardous Materials, 146, 255-261.

PARSHAKOV N.S., LAUBENBAKH A.I., SLAVYAGINA I.I. SKOSYREVA L.N., 1978, Features of distribution of radioactive elements in bauxite-bearing deposits, International Geology Review, 20(11), 1319-1329.

PARSHAKOV N.S., MENYAYLOV A.A., LAUBENBAKH A.I., SKOSYREVA L.N., SLAVYAGINA I.I., 1977, Radioactivity and mineral composition of bauxites. International Geology Review, 19(6), 737-740.

RUYTERS S., MERTENS J., VASSILIEVA E., DEHANDSCHUTTER B., POFFIJN A., SMOLDERS E., 2011, *The red mud accident in Ajka (Hungary): Plant toxicity and trace metal bioavailability in red mud contaminated soil*, Environmental Science & Technology 45: 1616-1622.

SAMAL S., ROY A.K., BANDHOPADDYAY A., 2013, *Proposal, resources and utilization of red mud in India-a review*, International Journal of Mineral Processing, 118, 43-55.

SOMLAI J., JOBBAGY V., KOVACS J., TARJAN S., KOVACS T., 2008, *Radiological aspects of the usability of red mud as building material additive*, Journal of Hazardous Materials, 150, 541-545.

ZHANG L., ZHANG H., GUO W., TIAN Y., 2014, *Removal of malachite green and crystal violet cationic dyes from aqueous solution using activated sintering process red mud*, Applied Clay Science, 93-94, 85-93.

ZHAO Y., WANG J., LIU C., LUAN Z., WEI N., LIANG Z., 2009, *Characterization and risk assessment of red mud derived from the sintering alumina process*, Fresenius Environmental Bulletin, 18(6), 989-993.